WOOD RESEARCH
61 (6): 2016
861-870

ESTIMATION OF ORTHOTROPIC MECHANICAL PROPERTIES OF WOOD BASED ON NON-DESTRUCTIVE TESTING

Lenka Melzerová, Lucie Kucíková, Tomáš Janda, Michal Šejnoha
Czech Technical University in Prague
Faculty of Civil Engineering, Department of Mechanics
Prague, Czech Republic

(Received December 2015)

ABSTRACT

This paper presents a simple approach for the derivation of effective properties of wood while accounting for its inherent anisotropy. These properties are found by combining the results of structural indentation using the Pilodyn 6J testing device and analytical homogenization in the framework of an inverse approach. This approach provides first a rough estimate of a microfibril angle and subsequently yields the predictions of the effective properties of wood. While applicable to any kind of wood we adopted the proposed methodology to spruce as a typical representative of soft wood. This allows us to exploit the presented results directly in the analysis of glued laminated timber beams made of spruce wood which is a principal goal of the present research.

KEYWORDS: Spruce wood, indentation, homogenization, microfibril angle.

INTRODUCTION

Natural wood belongs to a principal building material for many centuries and is still on a continuous rise even today in many areas of civil engineering. Among others, an application of glued laminated timber beams has been receiving a particular attention. A relatively high slenderness of such beams combined with a complex microstructure of wood calls for a proper material characterization. Accepting an orthotropic nature of wood then becomes a stepping stone in arriving at meaningful and reliable predictions of the behaviour of laminated timber beams at a structural level.

A considerable attention has been accorded to the derivation of effective macroscopic properties using various tools of analytical (Hofstetter et al. 2005, Šejnoha and Zeman 2013) or numerical (Vorel et al. 2015) homogenization. However, these predictions are strongly influenced by the microfibril angle (MFA) which is difficult to measure. Because of that, an inverse approach

combining anisotropic nanoindentation at the level of wood cell and analytical homogenization has been promoted as a promising tool to estimate MFA (Jäger et al. 2004). Unfortunately, such an approach goes usually beyond the facility of most engineering companies where the determination of material properties most often relies on classical laboratory tests. Here, the non-destructive testing based on indentation at the level of timber beam using, e.g. the Pilodyn 6J measuring device can be adopted to acquire the knowledge of the longitudinal (axial) elastic modulus (Melzerová et al. 2012) to be used in numerical analyses, see e.g. (Melzerová et al. 2015). While this method can directly be applied to the already constructed beams and thus account for the actual properties of wood it lacks information about the properties in the plane normal to the fiber direction. In this contribution, we overcome this obstacle by effectively combining the results provided by structural indentation and homogenization. At first glance, estimating MFA from macroscale experiments may seem less reliable in comparison to nanoindentation measurements. However, taking into account a number of uncertainties associated with nanoindentation, e.g. a low quality of indented surface to name at least one, the present approach appears sufficiently robust for the prediction of the effective properties of wood with a direct link to an engineering practice. Further improvement can be expected with the help of the Bayesian statistical method (Melzerová et al. 2015).

The rest of the paper is organized as follows. Following the introductory part we present in the next section the theoretical background for the evaluation of the effective longitudinal elastic modulus both from indentation and analytical homogenization including the estimation of the microfibril angle. The relevant results are discussed subsequently followed by the summary of the essential findings.

MATERIAL AND METHODS

This section outlines experimental and analytical approaches for the estimation of the effective longitudinal elastic modulus. The two approaches are then combined to provide estimates of MFA and consequently the effective properties of wood.

Statistical evaluation of macroscopic indentation

The Pilodyn 6J measuring device in Fig.1a was adopted to determine the longitudinal elastic modulus of spruce. The device shoots the indenter tip into the wood with a given energy and measures the indentation depth with 0.5 mm accuracy while simultaneously controlling the wood moisture. The measured depth is then linked to a local wood density. The required macroscopic longitudinal modulus of elasticity in the fiber direction (E_A in MPa) can be determined indirectly either from the wood density or from the measured indentation depth (t_p in mm) as

$$E_A = -564.1 t_p + 19367 \tag{1}$$

Note that Eq. 1 provides the longitudinal elastic modulus assuming that the indentation is performed more or less in the transverse direction, i.e. in the direction normal to the fiber orientation. Due to wood heterogeneity and the way individual segments of plies are cut from the trunk it appears advisable to check the influence of the indentation direction on the spruce wood response.

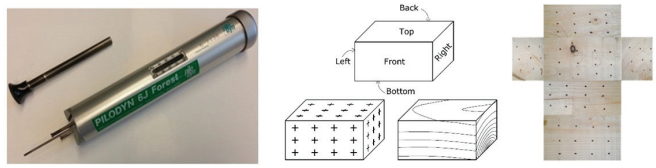

a) b) c)

Fig. 1: a) Pilodyn 6J testing device, b) Sketch of an indented sample with an identification of indented faces, c) Sample A showing indentation faces.

To that end, two samples of spruce denoted as A and B and having dimensions (width×height×length = 64×84×932 mm) were taken from two different locations of the supplied glued laminated beam, cut into 6 specimens and tested. Labelling of individual faces used in the subsequent statistical analysis is shown in Fig. 1b. Indentation directions with respect to the fiber orientation and growth rings are then evident from Fig. 1b, c. This allows us to associate the top and bottom faces with an indentation in the radial direction, the front and back faces with the tangential direction and the left and right faces with the longitudinal direction. In addition, the radial and tangential directions will be jointly referred to as transverse directions.

Evaluation of effective elastic properties from homogenization

Softwood is produced by conifer trees and manifests itself by a high degree of porosity represented mainly by hollow tubes called tracheids aligned axially in the tree. They account for more than 90 % of the total volume of the wood. The remainder is then taken by radially aligned rays. In woods with strong seasonal differences we clearly identify two types of tracheids within an annual ring forming the sections of earlywood and latewood, see Fig. 2a. As evident from Fig. 2b, the earlywood is characterized by rather thin walls surrounding larger holes called lumens having more or less square or polygonal cross-sections, while the latewood, see Fig. 2c, exhibits much thicker walls and thinner lumens with a rectangular cross-section elongated in the tangential direction.

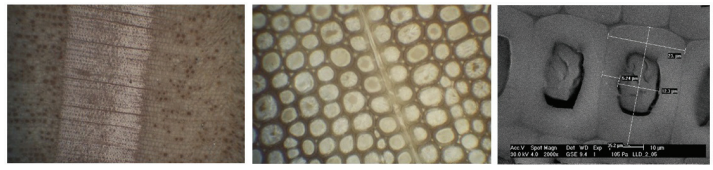

a) b) c)

Fig. 2: Transverse cross-section of spruce: a) microstructure of early and late wood provided by optical microscope, b) a detailed representation of early wood, c) a wood cell of a late wood provided by scanning electron microscope.

Regardless of the type of wood examined, the respective microstructural details above the cell wall can be well acquired from a standard image analysis and further utilized, e.g. in the mechanical modelling which in turn may benefit from the concept of hierarchical micromechanics (Hofstetter et al. 2005, Šejnoha and Zeman 2013). The present analysis builds upon the application of three-scale homogenization for softwood to get the estimates of overall macroscopic properties.

Below the cell wall level each wood is assumed to be represented by a composition of tissue independent properties mentioned in the preceding paragraph. The specific values of needed material parameters together with their volume fractions are available, e.g. in (Hofstetter et al. 2005). Following (Hofstetter et al. 2005, Šejnoha and Zeman 2013) the cell wall is visualized as a three-phase composite consisting of cylindrical fiber-like aggregates of crystalline and amorphous cellulose embedded into an isotropic polymer matrix. The matrix properties are found from an independent homogenization step comprising the properties and volume fractions of hemicellulose and lignin only, thus neglecting the presence of water and other wood extractives. In contrast to the analysis presented in (Hofstetter et al. 2005) we introduce an additional simplification by employing the Mori-Tanaka (Benveniste 1987) homogenization approach on all scales. The third homogenization step corresponds to the analysis of a homogeneous matrix constructed from the previous two-steps and weakened by aligned cylindrical pores. The volume fraction of the porous phase can be effectively estimated from binary images in Fig. 3 corresponding to a real microstructure in Fig. 2. The white colour represents the area of lumens amounting to a volume fraction equal to 0.56 for an earlywood and 0.27 for a latewood, respectively. At first three levels the 6 × 6 effective stiffness matrix $\mathbf{L}^{hom}$ and the effective compliance matrix $\mathbf{M}^{hom}$ provided by the Mori-Tanaka method are written as

$$\mathbf{L}^{hom} = [\sum_{r=1}^{N} c_r \mathbf{L}_r \mathbf{T}_r][\sum_{r=1}^{N} c_r \mathbf{T}_r]^{-1}, \mathbf{M}^{hom} = [\sum_{r=1}^{N} c_r \mathbf{M}_r \mathbf{W}_r][\sum_{r=1}^{N} c_r \mathbf{W}_r]^{-1} \tag{2}$$

where: c_r - the volume fraction of the phase r,
$\mathbf{L}_r$ and $\mathbf{M}_r$ -store the corresponding stiffnesses and compliance,
N - the number of phases,
$\mathbf{T}_r$ and $\mathbf{W}r$ - the partial strain and stress concentration factors depending on the shape of the inclusion and the properties of the matrix phase and follow from the solution of the Eshelby transformation inclusion problem.

For further details we refer the interested reader to (Benveniste 1987, Šejnoha and Zeman 2013).

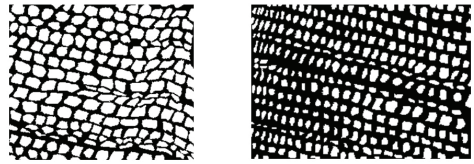

a) b)

Fig. 3: Binary image at the level of tracheids: a) earlywood – c_{lumens}= 0.56, b) latewood – c_{lumens}= 0.27.

A laminated structure of wood, the sequence of annual rings, is then exploited in the evaluation of the effective properties of wood in terms of the Voigt and Reuss bounds using the standard rules of mixture in the form

$$\mathbf{L}^{voigt} = c_{EW}\mathbf{L}^{EW} + c_{LW}\mathbf{L}^{LW}, \mathbf{M}^{reuss} = c_{EW}\mathbf{M}^{EW} + c_{LW}\mathbf{M}^{LW} \tag{3}$$

where: c_{EW}, c_{EM} stand for the volume fractions of the earlywood and latewood, respectively. The associated stiffness ($\mathbf{L}^{EW}$, $\mathbf{L}^{LW}$) and compliance ($\mathbf{M}^{EW}$, $\mathbf{M}^{LW}$) matrices are found from the 3rd homogenization step. See ahead Tab. 4 for a specific labelling of individual scales.

Estimating microfibril angle

Suppose that the microfibril angle MFA=β is defined as the angle between the x_1-axis parallel to lumens and a line x_β contained by a plane being perpendicular to the plane x_2x_3. The line x_β is aligned with the direction of the microfibrils and as such is associated with the longitudinal modulus E_A in Tab. 4. Note that MFA is defined within the plane tangential to the cell wall. We further accept that microfibrils are wound helically around the cell wall (Abrham and Elbaum 2013). This allows us to assume that there is no preferential plane x_1x_β which calls for orientation averaging to account for all the possible orientations of this plane. In case of discrete averaging the effective moduli at the cell wall level can be extracted from

$$\langle\langle \mathbf{M}^{2g} \rangle\rangle = \frac{1}{N}\sum_{i=1}^{N} \mathbf{M}^{2g}\left(\alpha^i, \beta, 0\right), \ \langle\langle \mathbf{L}^{2g} \rangle\rangle = \frac{1}{N}\sum_{i=1}^{N} \mathbf{L}^{2g}\left(\alpha^i, \beta, 0\right) \tag{4}$$

where: N → ∞ and $\langle\langle \mathbf{M}^{2g} \rangle\rangle$ $\langle\langle \mathbf{L}^{2g} \rangle\rangle$ are the compliance and stiffness matrices, respectively, associated with the 2nd homogenization step, recall Tab. 4, and transformed into the global coordinate system. In Eq. 4 α is the angle with which the global axis x_2 deviates from the tangential plane x_1x_β. The index i denotes the discrete value of α when averaging. Point out that in this case $\langle\langle \mathbf{M}^{2g} \rangle\rangle^{-1} \neq \langle\langle \mathbf{L}^{2g} \rangle\rangle$ in general. On the contrary, the two expressions are equivalent if performing the averaging within the framework of the Mori-Tanaka method, see e.g. (Vorel and Šejnoha 2009) for more details. It is also interesting to point out that the Mori-Tanaka predictions are almost identical to $\langle\langle \mathbf{L}^{2g} \rangle\rangle$.

Thus if we wish for the two expressions in Eq. 4 to provide the same estimates of effective properties we must search for two different microfibril angles β^M, β^L. When comparing Eqs. 3 and 4, we may associate the two angles with the lower $\beta^M \approx \beta^{LB}$ and upper $\beta^L \approx \beta^{UB}$ bound on MFA. The two values are found from the solution of the following minimization problems

$$min\left|E_A^{pilodyn} - E_A^{4a}(\beta^{LB})\right|, \quad min\left|E_A^{pilodyn} - E_A^{4a}(\beta^{UB})\right| \tag{5}$$

where: $E_A^{4a}(\beta^{LB})$ corresponds to the effective longitudinal Young modulus found from step 4 of the homogenization scheme when adopting the cell properties in the 3rd and 4th homogenization step given by Eq. 4_1. Similarly, $E_A^{4a}(\beta^{UB})$ follows from the application of Eq. 4_2. $E_A^{pilodyn}$ in Eq. 5 was set equal to 14 GPa, recall Tab. 3.

RESULTS AND DISCUSSION

This section presents the results found from the application of the proposed experimental-computational approach. A statistical evaluation of indentation measurements is discussed first addressing also the effect of indentation direction. The results of analytical homogenization in terms of the effective properties of wood under the assumption of zero MFA are summarized next opening a question about the influence of the microfibril angle. This issue is investigated last giving the final predictions of the properties of wood to be used in an independent structural analysis.

Statistical evaluation of macroscopic indentation results

The results of indentation in terms of averages and standard deviations of the indentation depth are summarized in Tab. 1. A graphical representation of the probability density functions corresponding to normal distribution is plotted in Fig. 4.

Tab. 1: Basic statistics of indentation depth t_p for two samples of spruce A/B.

Indentation direction	No. of indents	Mean (mm)	Standard deviation (mm)
Longitudinal	108	11.79/13.05	1.70/3.58
Radial	144	9.05/9.51	1.25/1.64
Tangential	144	8.98/9.55	1.27/2.07
Transverse	288	9.01/9.53	1.26/1.87

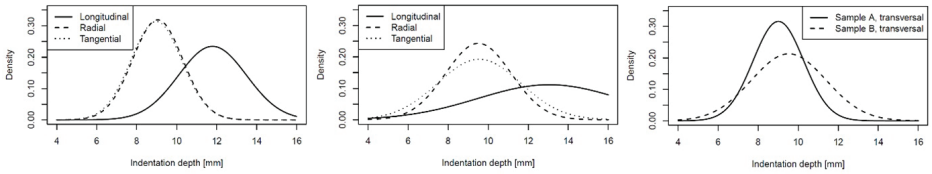

a) b) c)

Fig. 4: a) Sample A, b) Sample B, c) Sample A and B incorporating collectively the data for transverse direction.

It is clear that indentation along the fiber direction provides results which considerably differ from those pertinent to the radial and tangential directions. On the contrary, the latter two directions do not show a particular difference thus promoting them both for the prediction of the longitudinal elastic modulus. A higher variability of the axial indentations potentially linked to the fiber kinking during indentation thus precludes these data for the derivation of a fitting Eq. 1.

A similar conclusion can be drawn from standard statistical tests to explore, for example, whether the difference of the means of two data sets is significant. Here we adopt the Welch's t-test for significantly different means for samples with potentially different variances and unequal samples sizes. To proceed, determine the t statistics data for transverse direction and the degrees of freedom ν as

$$t = \frac{\overline{x_1} - \overline{x_2}}{\sqrt{\frac{s_1^2}{N_1} + \frac{s_2^2}{N_2}}}, \tag{6}$$

$$\nu \approx \frac{\left(\frac{s_1^2}{N_1} + \frac{s_2^2}{N_2}\right)^2}{\frac{s_1^4}{N_1^2(N_1-1)} + \frac{s_2^4}{N_2^2(N_2-1)}}, \tag{7}$$

where: x_i, s_i, N_i - the sample mean, variance estimate and population size of the i_{th} sample. Next, compute the significance p of t as the probability that t can be this large for distributions with equal means. It is found by integrating the Student's t probability distribution function from $-\infty$ to $|t|$. Therefore, a small value of p means that the observed difference is very significant and vice versa.

Clearly, the values of p listed in Tab. 2 suggests for both samples A and B that the mean difference for indentation data sets associated with radial and tangential directions is insignificant (the p value is relatively large), whereas for indentation data sets associated with longitudinal and transverse directions the mean difference is very significant (the p value is much smaller than any

Tab. 2: Welch's test for significantly different means.

Sample	$\|t\|$	v	p
Radial and tangential direction			
A	0.49	285.9	0.32
B	0.16	271.5	0.44
Axial and transverse direction			
A	15.4	153.0	3.03×10^{-33}
B	0.16	271.5	1.91×10^{-17}
Transverse direction for samples A and B			
A/B	3.91	503.8	5.30×10^{-5}

of the common significance levels). There is thus no difference between the radial and tangential direction and the indentation depths for both directions can be adopted in the fitting Eq. 1.

Although having only two samples, we finally compared, whether samples A and B have on average the same mechanical properties. By judging from Fig. 4c) this is not that obvious. On the other hand, a rather small value of the probability p stored in the last row of Tab. 2 confirms a significant difference, at least from the mathematical point of view, in the mean response of both samples. From other prospective, this final observation further suggests that even for a relatively large dispersion of data provided by the Pilodyn testing device, this measuring technique makes it possible to uncover differences in mechanical properties of individual ply segments used to build the laminated timber beams. This is partly seen in the calculated statistics of the longitudinal modulus found for both samples using Eq. 1 and all the measurements collected in the transverse direction, see Tab. 3. Nevertheless, from the structural applications point of view and realizing the already mentioned measuring precision, this difference is negligible.

Tab. 3: Basic statistics of longitudinal elastic modulus E_A of spruce.

Sample	No. of indents	Mean (GPa)	Standard deviation (GPa)
A	288	14.3	0.71
B	288	13.9	1.05

Evaluation of effective elastic properties from homogenization - results

Unlike the indentation method the theory of analytical homogenization provides the entire stiffness and compliance matrices. These follow from the application of Eqs. 2 and 3. In particular, the homogenized properties pertinent to individual scales up to the level of tracheids follow from Eq. 2 and are summarized in Tab. 4, the homogenization steps 1-3. Eq. 3 is then called to yield the effective properties of the entire wood, the homogenization step 4.

Estimating microfibril angle-results

As evident from Tab. 4, we arrive in case of MFA = 0° at the ratio of longitudinal and transverse modulus around 10. However, in such a case the estimated longitudinal modulus E_A^{voigt} is significantly higher than the measured one. This becomes evident by comparing the results in Tabs. 3 and 4. Such a difference thus suggests a non-zero MFA which clearly affects the ratio of these moduli. A simple approach in which we attempt to match the measured E_A and the predicted one E_A^{voigt} as a function of MFA was presented in the previous section. Thus if introducing $E_A^{pilodyn}$ =14 GPa in Eq. 5 we obtain the results stored in Tab. 5.

Tab. 4: Effective elastic properties from four-step homogenization.

Step No.	E_A	G_A	ν_A	E_T	G_T	ν_T	E_A/E_T
1 - Polymer network	6.89	2.60	0.32	6.89	2.60	0.32	1.00
2 - Cell wall	42.34	2.91	0.25	9.23	2.74	0.42	4.86
3a - Earlywood	18.37	0.81	0.25	1.83	0.63	0.33	10.04
3b - Latewood	30.82	1.57	0.25	4.28	1.40	0.36	7.20
4a - Wood Voigt	22.32	1.08	0.25	2.53	0.92	0.37	8.83
4b - Wood Reuss	21.06	0.96	0.25	2.17	0.80	0.36	9.70
Lamination theory - step 4	c_{EW}		c_{LW}		E_A^{voigt}/E_T^{reuss}		
	0.68		0.32		10.29		

Tab. 5: Numerically estimated range of MFA.

$MFA=\beta^{LB}$	$MFA=\beta^{UB}$	E_A^{voigt}/E_T^{reuss}
13	25	6.6

Recall that at present we do not search for the bounds on effective properties. For the two values of the microfibril angle provided by Eq. 5 the effective properties, and thus also the ratio of longitudinal and transverse moduli, are identical. The specific values to be used in a structural analysis are available in Tab. 6.

Tab. 6: Effective elastic properties for MFA≠ 0°.

E_A	G_A	ν_A	E_T	G_T	ν_{AT}
14.05	2.05	0.31	2.14	0.79	0.35

It should be stressed that the proposed range of the microfibril angle follows purely from numerical analysis. On the other hand, it may be ascribed to a high variability of this quantity as its specific value depends on several factors such as the tree growth rate, the tree age, location of the cell within the tree trunk, etc. As for the spruce the literature offers values ranging from MFA=0° to MFA=50°, see e.g. (Gindl et al. 2004). For the tested wood the proposed range of MFA can therefore serve as a stepping stone in the Bayesian statistical method. The prior distribution of MFA will be updated utilizing the knowledge of effective properties from an independent experimental program, say from tensile tests on flat wood samples having thickness of just a few growth rings. These results will be presented in (Šejnoha et al. 2017).

CONCLUSIONS

The paper concentrates on the application of the Pilodyn 6J testing device to calculate the longitudinal elastic modulus from the measured depth of macroscopic indents. It has been shown that for a sufficiently large number of indents this non-destructive testing method is capable of distinguishing the mechanical properties of various types of samples of the same kind of wood. This is particularly advantageous in conjunction with the laminated timber structures where the variability of individual segments between two finger joints may be quite significant.

Unfortunately, this simple testing method does not give any information about the material anisotropy, which on the other hand may play a crucial role in the prediction of mechanical response of high, generally heterogeneous, laminated timber beams. Here, the combination of

these easy to perform measurements and analytical homogenization appears as a suitable method of attack. If assuming that microfibrils of the crystalline cellulose are perfectly aligned with the direction of lumens we arrived for the tested samples of spruce at the ratio of the longitudinal and transverse direction equal approximately to 10. This assumption, however, considerably overestimated the macroscopic longitudinal stiffness of wood derived from homogenization. This discrepancy is often blamed on a non-zero value of microfibril angle. In this paper the Pilodyn measurements were exploited to estimate the possible range of MFA and consequently to predict the complete homogenized anisotropic stiffness matrix of the wood. For the present case the predicted values of MFA amounted to 13° and 25° depending on the type of Eq. 4 used in the orientation averaging. This step further reduced the ratio of longitudinal and transverse moduli to about 7. Such a result may open the question about the reliability of the homogenization procedure, or rather the reliability of the material data used on microscale, since the literature often reports this ratio close to 30, but with very limited information on how the measurements in transverse direction were carried out.

ACKNOWLEDGMENTS

This outcome has been achieved with the financial support of the Ministry of Education, Youth and Sports of the Czech Republic, project No. LD12023 advanced methods for design, strengthening and evaluation of glued laminated timber. The support by the GAČR grant No. 15-10354S is also gratefully acknowledged.

REFERENCES

1. Abraham, Y., Elbaum, R., 2013: Quantification of microfibril angle in secondary cell walls at subcellular resolution by means of polarized light microscopy. New Phytologist 197(3): 1012-1019.
2. Benveniste, Y., 1987: A new approach to the application of Mori-Tanaka theory in composite materials. Mechanics of Materials 6(2): 147-157.
3. Gindl, W., Gupta, H., Schoberl, T., Lichtenegger, H., Fratzl, P., 2004: Mechanical properties of spruce wood cell walls by nanoindentation. Applied Physics A: Applied Science and Processing 79(8): 2069-2073.
4. Hofstetter, K., Hellmich, C., Eberhardsteiner, J., 2005: Development and experimental validation of a continuum micromechanics model for the elasticity of wood. European Journal of Mechanics - A/Solids 24(6): 1030-1053.
5. Jäger, A., Bader, T., Hofstetter, K., Eberhardsteiner, J., 2004: The relation between indentation modulus, microfobril angle, and elastic properties of wood cell walls. Composites: Part A 35(11): 1345-1349.
6. Melzerová, L., Janda, T., Šejnoha, M., Šejnoha, J., 2015: FEM Models of glued laminated timber beams enhanced by Bayesian updating of elastic moduli. International Journal of Mechanical, Aerospace, Industrial and Mechatronics Engineering 9(5): 599-605.
7. Melzerová, L., Kuklík, P., Šejnoha, M., 2012: Variable local moduli of elasticity as inputs to FEM-based models of beams made from glued laminated timber. Technische Mechanik 32(2-5): 425-434.

8. Vorel, J., Sýkora, J., Urbanová, S., Šejnoha, M., 2015: From CT scans of wood to finite element meshes. B. Topping (Editor). In: Proceedings of the The Fifteenth International Conference on Civil, Structural and Environmental Engineering Computing, Prague, Czech republic, Civil-Comp Press, Stirlingshire, UK, Paper 221, 2015. doi: 10.4203/ccp.108.221, ISSN 1759-3433.
9. Vorel, J., Šejnoha, M., 2009: Evaluation of homogenized thermal conductivities of imperfect carbon-carbon textile composites using the Mori-Tanaka method. Structural Engineering and Mechanics 33(4): 429-446.
10. Šejnoha, M., Zeman, J., 2013: Micromechanics in Practice. WIT Press, Southampton, Boston, 271 pp.
11. Šejnoha, M., Janda, T., Vorel, J. Kucíková, L. Padevět, P., 2017: Combining homogenization, indentation and Bayesian inference in estimating the microfibril angle of spruce. In: Procedia Engineering, Structural and Physical Aspects of Construction Engineering.

*Lenka Melzerová, Lucie Kucíková, Tomáš Janda, Michal Šejnoha
Czech Technical University in Prague
Faculty of Civil Engineering
Department of Mechanics
Thákurova 7/2077
166 29 Praha 6
Czech Republic
Corresponding author: melzerov@fsv.cvut.cz